Stochastic Dynamical Response of a Gear Pair under Filtered Noise Excitation

Saeed Gheisari Hasnijeh[a,1], Arvid Naess[b], Mehrdad Poursina[a], Hossein Karimpour[a]

[a] *Department of Mechanical Engineering, University of Isfahan, Isfahan, Iran*
[b] *Department of Mathemsatical Sciences, Norwegian University of Science and Technology, Trondheim, Norway*

Abstract

In this study, the stochastic dynamic response of a spur gear pair model under the excitation of filtered noise is investigated. The spur gear pair is modeled as a single degree of freedom (SDOF) system in which nonlinear and non-smooth backlash and time-varying mesh stiffness as well as stochastic excitation are concurrently considered. Four cases are addressed, based on how the noise is incorporated in the loading terms. A first order filter is employed to generate various filtered noises with the same energy but different power spectrum. The combination of the SDOF gear model and the shaping filter leads to a (3D) Markov model. The numerical path integration (PI) technique is adopted to obtain the probabilistic response of the gear model using an adaptive time-stepping method in order to increase the accuracy of the time integration. A 4D system is also considered by applying a second order filter to model a narrow-band noise. The results are verified by comparing with Monte Carlo simulations. The effect of the noise spectrum on the probabilistic response is evaluated for different loading cases. The response PDF is of key importance in relation to reliability assessment of gear systems.

Keywords: non-smooth gear model, stochastic dynamics, path integration, filtered noise

[1] Corresponding author. Tel.: +98 9132127349.
E-mail address: saeed.gheisari@gmail.com

1. Introduction

Gears are widely used in different applications within a range of various industries. Investigation on the dynamical behavior of gears is fundamental for studying other fields of related research such as design, tribology, reliability assessment, etc. The first studies attempting to investigate the dynamics of gear systems originated in the early 20th century and the topic has continued to be a very active research area until now. Early gear models were linear, excluding or neglecting nonlinearities such as backlash [1]. Nonlinear, time-varying (NTV) gear models were developed and investigated in the 90's [2–5]. More recently, researches have focused on multi-degrees of freedom (DOF) modeling of the gear mesh system, which lead to more realistic and complicated models as well [6,7]. All those studies belong to the category of deterministic dynamics.

Stochastic excitation may be prevalent in gear systems due to randomness in the external loading or within internal parameters. In some applications, such as wind turbine drivetrains, ship propulsions and automobile gearboxes, the effect of randomness is significant, which implies the necessity to conduct a stochastic analysis to obtain accurate and realistic results. Moreover, knowledge about the probability density function (PDF) of the response is of key importance for the purpose of reliability assessment and reliability-based design in such systems. This latter can be achieved by considering a stochastic component as part of the excitation. Under suitable modelling assumptions, this would typically lead to a stochastic differential equation (SDE). Although the simplest stochastic excitation is the Gaussian white noise (GWN), which is characterized by a uniform power across the frequency band, real stochastic loadings will invariably have varying spectral distributions. For instance, some wind loadings has a descending power spectral density (PSD) which can be approximated by a first order linear filter [8]. In this work, the random excitation is assumed to be a filtered Gaussian white noise, enabling us to express the SDE in the state space as an n-dimensional problem. The response of such systems is a Markov vector process and its transitional PDF is governed by the Fokker-Planck (FP) equation. However, the analytical solution of the FP equation is restricted to linear systems and a limited class of nonlinear models [9].

The pioneering studies of Tobe et al. [10,11] considered random excitation in gear systems using a statistical linearization technique. They also experimentally verified their theoretical results. Based on the fact that using statistical linearization leads to inaccurate results for systems with discontinuous nonlinearities, Kumar et al. [12] adopted a direct integration technique to study the dynamic response of a gear pair. Similarly, Neriya et al. [13] investigated a helical gear system which included both backlash and time-varying mesh stiffness, and was also subjected to a random transmission error. The mean value and variance of the response were calculated by the piecewise linearization method. Pfeiffer and Kunert [14] evaluated the rattling problem for a gear system. Wang and Zhang [15] considered the effect of speed-dependent random errors on the stochastic vibration of the gear model. These contributions in the field of stochastic gear dynamics have been very valuable in terms of the relative impact and perspective they have given, regardless of their accuracy and efficiency.

A numerical approach to approximate the solution of FP equations is provided by the path integration (PI) method. Among the first to apply this method was Wehner and Wolfer [16], who used it to solve simple, nonlinear FP equations. Subsequently, Naess and Moe [17], Lin and Yu [18], Zhu [19], and others, have applied and further developed the PI technique in order to evaluate several engineering problems. The application of the path integration method is limited to Markov systems subjected to multiplicative or additive noise. An efficient and accurate approach was applied by Naess et al. [20] for solving a SDOF non-smooth gear model under stochastic excitation caused by Gaussian white noise. The dynamical model was assumed as nonlinear time-invariant (NTI), neglecting the variation of mesh stiffness with contact status. They adopted a short time Gaussian approximation (STGA) to approximate the conditional PDF [21] and captured the evolution of the response PDF using a stepwise solution technique. Later, Mo and Naess [22] showed that the stochastic and deterministic attractors are very similar by comparing the response PDF with the Poincaré map of the deterministic system in Ref. [2]. In both papers, a fixed time step was used in general. However, in order to reduce numerical errors due to non-smooth dynamical behavior, a backward Runge-Kutta time-stepping algorithm combined with a Newton iteration method was used to split the fixed step into two sub-steps. This permits to accurately determine when the deterministic trajectory crosses the boundary between two regimes of nonlinearity. Another similar approach to account for the piecewise backlash function was

proposed by Wen et al. [23], who dealt with a linear dynamic model for each part of the state space. Although an important interaction between time-varying mesh stiffness and backlash nonlinearity in gear meshing systems was reported, a constant averaged stiffness was used in their model. Considering the stochasticity of the system, establishing the exact switching time between different regimes of the dynamical system is not meaningful since there is no deterministic trajectory. Therefore, the aforementioned approach may fail to be sufficiently accurate and efficient, a fact confirmed by the results obtained with Monte Carlo simulations. In order to decrease the calculation error, Hasnijeh et al. [24] applied a novel adaptive scheme time-stepping method. The main idea of this method is to determine the time-step length based on the amount of marginal probability at non-smooth boundaries. The authors demonstrated the efficiency of the adaptive relative to the fixed time-stepping for non-smooth systems.

A point that is not always fully appreciated in the literature, is that the numerical solution of a SDE by necessity relies on discretization. This implies that the associated path integral (cf. Eq. (19)) represents the exact solution of the discretized SDE. The level of accuracy obtained in the representation of this exact solution, of course, depends on the numerical procedures implemented to calculate the path integral, cf. subsection 5.2. It is also worth mentioning, that in recent years efforts have been pursued to follow another line of approach to the path integral idea for stochastic structural dynamics [25,26]. It is based on a functional representation of the path integral in the spirit of the Feynman path integral in quantum mechanics.

Monte Carlo simulation (MCS) is the simplest and usually the most reliable approach to determine the response PDF of SDEs. In this approach, the response statistics are extracted from a large number of response realizations, which are generated using a stochastic integration method. Feng et al. [27] used MCS to investigate a stochastic spur gear model including the effects of sliding friction. It is worth mentioning that MCS is typically used as a verification tool for checking results obtained by other more efficient methods. In comparison, it is a rather time-consuming method if highly accurate results are needed, especially for low probability events.

In the current study, the response PDF of an SDOF nonlinear, time-varying gear model under the excitation of a filtered noise is obtained. The NTV gear model includes both backlash

nonlinearity and time-varying mesh stiffness (TVMS). Three main sub-problems are addressed herein. The first assignment consists to prove the capability of the adaptive path integration (API) method to investigate non-smooth dynamical gear systems under the excitation of filtered white noise. A first order filter is used to generate filtered white noise, extending the Markov property of this second-order system to the 3D state space. The second goal pursued here is to evaluate the effect of uncertain loading parameters on the response PDF. For this purpose, the additive noise infiltration into the problem is categorized into four different stochastic loading cases. Finally, a parametric study is carried out to show the effect of the loading spectrum on different aspects of the response PDF. Three filtered versions of noises are applied with equal energies but different spectrum distributions. To assess the capability of the path integration method in dealing with systems of higher dimensions, a 4D system is also considered by using a second-order filter to generate a narrow-band noise. As well as for the 3D problem, the effect of the loading spectrum on different aspects of the response PDF is investigated. Results are verified by Monte Carlo simulations for all cases. To the best of the authors' knowledge, the response PDF of a non-smooth gear model under filtered noise has not been investigated before. The response PDF contains a lot of raw information which can be utilized in different ways depending on the purpose of the analysis, such as mechanical design and reliability analysis. In addition, the effect of the input frequency spectrum on the response PDF is studied for each stochastic excitation case.

2. Stochastic dynamical model

A spur gear pair model is considered as shown in Fig 1. The corresponding equation of motion is given in dimensionless form and its derivation is briefly presented in the Appendix or through Ref. [24].

$$\ddot{q}(t) + 2\zeta\dot{q}(t) + k_h(t)f\big(q(t)\big) = F_m + F_{ah}\cos(\Omega t) \tag{1}$$

$$f\big(q(t)\big) = \begin{cases} q(t) - 1 & q(t) > 1 \\ 0 & -1 < q(t) < 1 \\ q(t) + 1 & q(t) < -1 \end{cases} \tag{2}$$

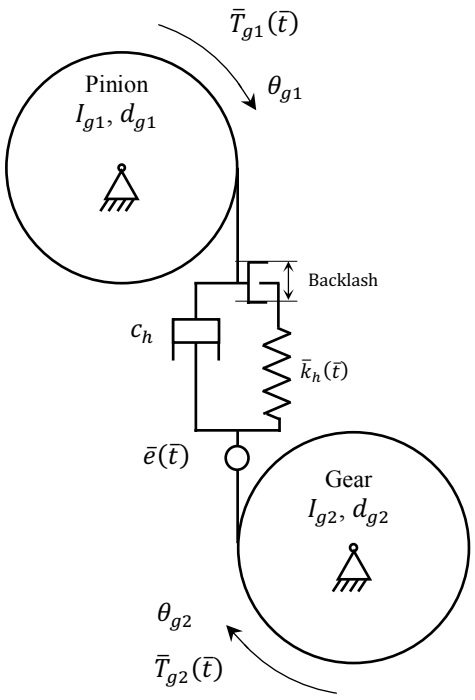

Fig. 1. Gear pair model [24]

In the dimensionless equation (1), q is the difference between the dynamic transmission error and the static transmission error, ζ denotes damping ratio, k_h is the time-varying mesh stiffness, f represents the nonlinear backlash function, Ω is the excitation frequency, and F_m and F_{ah} are the mean and alternating components of the loading, respectively.

Equation (1) is a two-dimensional state space NTV problem and may have multi-solutions, depending on the parameter values. The deterministic solution of this system can include no-impact, single-sided or double-sided impact cases, maybe with several subharmonics [2]. In the case of a multi-solution problem, the initial conditions will determine which deterministic solution would occur. As opposed to deterministic dynamics, the probabilistic response of the system may include both solution types simultaneously because of the stochastic essence of the excitation and also due to uncertain initial conditions [23]. In order to evaluate the effect of uncertainty in loading components on the dynamical behavior of the gear system, four separate cases are defined in the following based on an additive noise F_s (with intensity λ).

Case A: Uncertainty in the mean component of the loading which may arise from external torque fluctuation

$$\ddot{q}(t) + 2\zeta\dot{q}(t) + k_h(t)f\big(q(t)\big) = (F_m + \lambda F_s) + F_{ah}{\Omega_h}^2\cos(\Omega_h t) \tag{3}$$

Case B: Uncertainty in the alternating component of the loading that may be caused by manufacturing errors [28–30]

$$\ddot{q}(t) + 2\zeta\dot{q}(t) + k_h(t)f\big(q(t)\big) = F_m + (F_{ah} + \lambda F_s){\Omega_h}^2\cos(\Omega_h t) \tag{4}$$

Case C: Uncertainty in the frequency of the alternating loading due to manufacturing errors or vacillation in gear rotational speed

$$\ddot{q}(t) + 2\zeta\dot{q}(t) + k_h(t)f\big(q(t)\big) = F_m + F_{ah}{\Omega_h}^2\cos\big((\Omega_h + \lambda F_s)t\big) \tag{5}$$

Case D: Uncertainty in the phase of the alternating loading that may arise from manufacturing error [28–30]

$$\ddot{q}(t) + 2\zeta\dot{q}(t) + k_h(t)f\big(q(t)\big) = F_m + F_{ah}{\Omega_h}^2\cos(\Omega_h t + \lambda F_s) \tag{6}$$

3. Filtered white noise

3.1. First order linear filter

The noise component is assumed to be a stationary process, allowing the use of the shaping filter techniques in order to generate it from a Gaussian white noise [31]. In this study, the stochastic excitation is considered to have a particular power spectral density (PSD) function which can be modeled as follows

$$\dot{F}_s = -\alpha F_s + \gamma N_t \tag{7}$$

where N_t is the standard Gaussian white noise process and, α and γ are filter parameters. Knowing that $N_t dt = dW(t)$ [32] and defining $x_1 = q(t)$, $x_2 = \dot{q}(t)$ and $x_3 = F_s(t)$, the state space form of equation (3) can be rewritten as

$$\begin{cases} \mathrm{d}x_1 = x_2 \mathrm{d}t \\ \mathrm{d}x_2 = \left[F_m + F_{ah}{\Omega_h}^2 \cos(\Omega_h t) - 2\zeta x_2 - k_h(t) f(x_1) + \lambda x_3\right] \mathrm{d}t \\ \mathrm{d}x_3 = -\alpha x_3 \mathrm{d}t + \gamma \, \mathrm{d}W(t) \end{cases} \tag{8}$$

where $W(t)$ now denotes a standard Wiener process with stationary and independent increments. Similar forms will be obtained for Eqs. (4), (5) and (6). The power spectral density function for F_s is considered as follows,

$$S(\omega) = \frac{\gamma^2}{2\pi(\omega^2 + \alpha^2)} \tag{9}$$

3.2. Second order linear filter

In order to evaluate the capability of the path integration method in dealing with non-smooth systems of higher dimensions, the gear model in combination with a second order linear filter is also considered. The filter equations are as follows [31]

$$\begin{cases} \dot{G}_s = -\alpha F_s \\ \dot{F}_s = G_s - \beta F_s + \gamma N_t \end{cases} \tag{10}$$

α, β and γ are filter parameters. In the current study, the second order filter is only used for case A. Defining $x_3 = G_s$ and $x_4 = F_s$, the 4D state space model for equation (3) can be written as

$$\begin{cases} \mathrm{d}x_1 = x_2 \mathrm{d}t \\ \mathrm{d}x_2 = \left[F_m + F_{ah}{\Omega_h}^2 \cos(\Omega_h t) - 2\zeta x_2 - k_h(t) f(x_1) + \lambda x_4\right] \mathrm{d}t \\ \mathrm{d}x_3 = -\alpha x_4 \mathrm{d}t \\ \mathrm{d}x_4 = (x_3 - \beta x_4) \mathrm{d}t + \gamma \, \mathrm{d}W(t) \end{cases} \tag{11}$$

The power spectral density function for F_s is obtained as follows,

$$S(\omega) = \frac{1}{2\pi} \frac{\gamma^2 \omega^2}{(\alpha - \omega^2)^2 + (\beta\omega)^2} \tag{12}$$

4. The path integration method

Equation (8) can be expressed by the standard Itô SDE form as follows,

$$\mathrm{d}\mathbf{x}(t) = \boldsymbol{\alpha}(\boldsymbol{x}, t)\mathrm{d}t + \boldsymbol{\beta}(t)\mathrm{d}\mathbf{W}(t) \tag{13}$$

Since the main goal of the current study is to investigate 3D problems, the formulation is developed for a 3D state space model. The formulation can be easily generalized to higher dimensions. Therefore, $\mathbf{x}(t) = (x_1, x_2, x_3)^{\mathrm{T}}$ is a 3D state space vector process, $\boldsymbol{\alpha}(\mathbf{x}, t)$ is the drift vector and $\boldsymbol{\beta}(t)$ is the diffusion matrix and the vector $\mathrm{d}\mathbf{W}(t) = \mathbf{W}(t + dt) - \mathbf{W}(t)$ denotes the independent increments of a standard Wiener vector process. The SDE (13) has a unique solution in the strong sense for every set of parameter values [33]. This solution has a joint probability distribution of states for a specific time that can be calculated through application of the numerical PI method.

The response of the dynamical system (13) is a Markov process and the transition probability density function (TPDF), $p(\mathbf{x}, t|\mathbf{x}', t')$, satisfies the Fokker-Planck (FP) equation, which is written as follows

$$\frac{\partial}{\partial x}p(\mathbf{x}, t|\mathbf{x}', t') = -\sum_{i=1}^{3}\frac{\partial}{\partial x_i}\alpha_i(\mathbf{x}, t)p(\mathbf{x}, t|\mathbf{x}', t') + \frac{1}{2}\sum_{i=1}^{3}\sum_{j=1}^{3}\frac{\partial^2}{\partial x_i \partial x_j}\left(\boldsymbol{\beta}(t).\boldsymbol{\beta}^{\mathrm{T}}(t)\right)_{i,j}p(\mathbf{x}, t|\mathbf{x}', t') \tag{14}$$

In addition to several numerical methods presented for solving the FP equation directly, the probabilistic evolution of the state space vector process $\mathbf{x}(t)$ can be captured based on the Markov property of the response using the basic equation of the PI method

$$p(\boldsymbol{x}, t) = \int_{\boldsymbol{\Gamma}} p(\boldsymbol{x}, t|\boldsymbol{x}', t')p(\boldsymbol{x}', t')d\boldsymbol{x}' \tag{15}$$

where $\boldsymbol{\Gamma}$ is the state space and $d\mathbf{x}' = \prod_{i=1}^{3} dx_i'$. In fact, the method consists of evaluating the TPDF core thence determining the PDF $p(\mathbf{x}, t)$ of the state space vector $\mathbf{x}$ at time t from the previous PDF $p(\mathbf{x}', t')$ at time t' through equation (15). To implement the PI method, a discrete time approximation is needed. Naess and Moe [17] proposed a fourth-order Runge-Kutta-Maruyama (RKM) for the numerical solution of (13) as follows

$$\mathbf{x}(t) = \mathbf{x}(t') + \mathbf{r}(\mathbf{x}(t'), t', \Delta t) + \beta(t')\Delta\mathbf{W}(t') \tag{16}$$

The deterministic part of equation (16) is the explicit fourth-order Runge–Kutta (RK4) approximation $\mathbf{x}(t) = \mathbf{x}(t') + \mathbf{r}(\mathbf{x}(t'), t', \Delta t)$, which represents the time evolution of the deterministic part of (13) with a global error of order $O(\Delta t^5)$, where $\Delta t = t - t'$. Numerical experiments predict that the approximation to the deterministic part outweighs other residues in terms of accuracy in the solution of Eq. (15) [32]. Thus, a fourth-order RKM is applied in the form of $\mathbf{r}(\mathbf{x}(t'), t', \Delta t)$ for the deterministic part of equation (13). The Wiener process $\mathbf{W}(t)$ has independent increments, hence $\Delta\mathbf{W}(t') = \mathbf{W}(t) - \mathbf{W}(t')$ is a Gaussian variable and the TPD $p(\mathbf{x}, t|\mathbf{x}', t')$ is a Gaussian PDF for every t'. For sufficiently small Δt, the time sequence $\{\mathbf{x}(t_i)\}_{i=0}^{\infty}$ becomes a Markov chain which can approximate the time-continuous Markov solution of the SDE (13). For the model given by Eq. (8), the conditional PDF $p(\mathbf{x}, t|\mathbf{x}', t')$ follows a degenerate multidimensional Gaussian PDF [34],

$$p(\mathbf{x}, t|\mathbf{x}', t') = \delta\big(x_1 - x_1' - r_1(\mathbf{x}(t'), t', \Delta t)\big)\, \delta(x_2 - x_2' - r_2(\mathbf{x}(t'), t', \Delta t))\, \tilde{p}(x_3, t|\mathbf{x}', t') \tag{17}$$

where $\delta(.)$ denotes the Dirac delta function and

$$\tilde{p}(x_3, t|\mathbf{x}', t') = \frac{1}{\sqrt{2\pi\gamma^2\Delta t}} \exp\left\{-\frac{(x_3 - x_3' - r_3(\mathbf{x}(t'), t', \Delta t))^2}{2\gamma^2\Delta t}\right\} \tag{18}$$

in which $r_{\mathrm{i}}(\mathbf{x}', t', \Delta t)$ $i = 1,2,3$ are Runge-Kutta increments corresponding to each state. If the initial PDF $p_0\big(\mathbf{x}^{(0)}\big) = p(\mathbf{x}, t_0)$ is specified, equation (15) can be written in a stepwise format as follows

$$p\big(\mathbf{x}^{(n)}, t_n\big) = \int_{\mathrm{R}^3} \dots \int_{\mathrm{R}^3} \prod_{i=1}^{n} p\big(\mathbf{x}^{(i)}, t_i|\mathbf{x}^{(i-1)}, t_{i-1}\big)\, p_0\big(\mathbf{x}^{(0)}\big)\, \mathrm{d}\mathbf{x}^{(0)} \dots \mathrm{d}\mathbf{x}^{(n-1)} \tag{19}$$

Equation (19) expresses the mathematical formulation of the PI technique as used in this study. A finite region of integration that covers almost the whole probability range of the response should be introduced for evaluating equation (19), with consideration that the computational time is dramatically influenced by the state space discretization resolution. If the region of integration is determined appropriately, the probability loss that arises would be negligible. The initial PDF can,

in principle, be chosen quite arbitrarily as long as there is nonzero variance in all spatial dimensions. This is necessary for the numerical algorithms to work properly. What determines the choice of the initial PDF depends on the specific problem investigated. For the purpose of this paper, the initial PDF is assumed to be Gaussian, as follows:

$$p_0\left(\mathbf{x}^{(0)}\right) = p\left(\mathbf{x}^{(0)}, t_0\right) = \prod_{i=1}^{n} \frac{1}{\sqrt{2\pi}\sigma_{x_i}^{(0)}} \exp\left(-\frac{1}{2}\left(\frac{x_i - \mu_{x_i}^{(0)}}{\sigma_{x_i}^{(0)}}\right)^2\right) \tag{20}$$

where $\mu_{x_i}^{(0)}, i = 1,2,3$ denote initial mean values and $\sigma_{x_i}^{(0)} (> 0), i = 1,2,3$ represent standard deviations.

A challenging issue in the numerical calculations of non-smooth dynamics is the abrupt change in their behavior. In the deterministic problems, it can be overcome by identifying the transition point between two different dynamical regimes within a time step and splitting it into two sub-steps with different dynamics. However, in the corresponding stochastic dynamic analysis, there is no specific trajectory that would allow the transition points to be identified. In this study, a new adaptive time-stepping scheme is used in order to reduce both the numerical error and calculation runtime in comparison with the fixed time-step method [24]. The main idea behind this adaptive time-stepping method is to decrease the time step proportionally to the magnitude of the marginal probability density at the non-smooth boundaries. In the considered gear system, there are two boundaries $x_1 = -1$ and $x_1 = 1$ that separate three different dynamical zones. The mathematical formulation behind this approach can be written as follows

$$\Delta t_i = t_i - t_{i-1} = \max\left[\left(\left(1 - \frac{\max\{p_{x_1}(-1, t_{i-1}), p_{x_1}(1, t_{i-1})\}}{p_{x_1}^{(\max)}}\right)\Delta t_{\max}\right), (\Delta t_{\min})\right] \tag{21}$$

where p_{x_1} is the marginal PDF for the state variable x_1 and $p_{x_1}^{(\max)}$ is its maximum value. $\Delta t_{\max}$ is the maximum time step, and a minimum time increment $\Delta t_{\min}$ is introduced in order to avoid a zero length step when the marginal PDF approaches its maximum at the specified boundaries.

5. Results and discussion

5.1. Deterministic dynamical behavior

The deterministic dynamics of the model is investigated in order to compare probabilistic response with the deterministic results. A square-wave is considered as follows

$$k_h(t) = \begin{cases} 0.8 & (n-1)t_p \le t < (n-1)t_p + t_p/2.\ \ n = 1.2.3\cdots \\ 1.2 & (n-1)t_p + t_p/2 \le t < nt_p.\ \ n = 1.2.3\cdots \end{cases} \quad (22)$$

where t_p is the gear mesh period. It has been reported that the interaction between time-varying mesh stiffness and backlash nonlinearity becomes more pronounced in the multi-solution zone and especially for heavily loaded systems [3]. As a dimensionless case of study, parameters $\zeta = 0.05$, $F_m = 0.3$ and $F_{ah} = 0.1$ are borrowed from references [2,3,23]. This is a heavily loaded gear pair system, since $\hat{F} = F_m/F_{ah} = 3$ [2]. For $\Omega_h = 0.65$ there are two coexisting solutions, which are named by Kahraman [2] as the no impact and the single-sided impact solutions (Fig.2-**Error! Reference source not found.**a). The deterministic domain of attraction is shown in (Fig 2-b). The deterministic system will adopt one of the solutions depending on the initial condition. The initial distribution parameters in this paper are chosen as $\mu_{x_1}^{(0)} = \mu_{x_2}^{(0)} = 0$, $\sigma_{x_1}^{(0)} = 0.5$ and $\sigma_{x_2}^{(0)} = 0.25$ which covers both basins of attraction, but mostly the single-sided impact solution. The difference between applying deterministic versus stochastic initial condition is illustrated schematically in Fig.2-b.

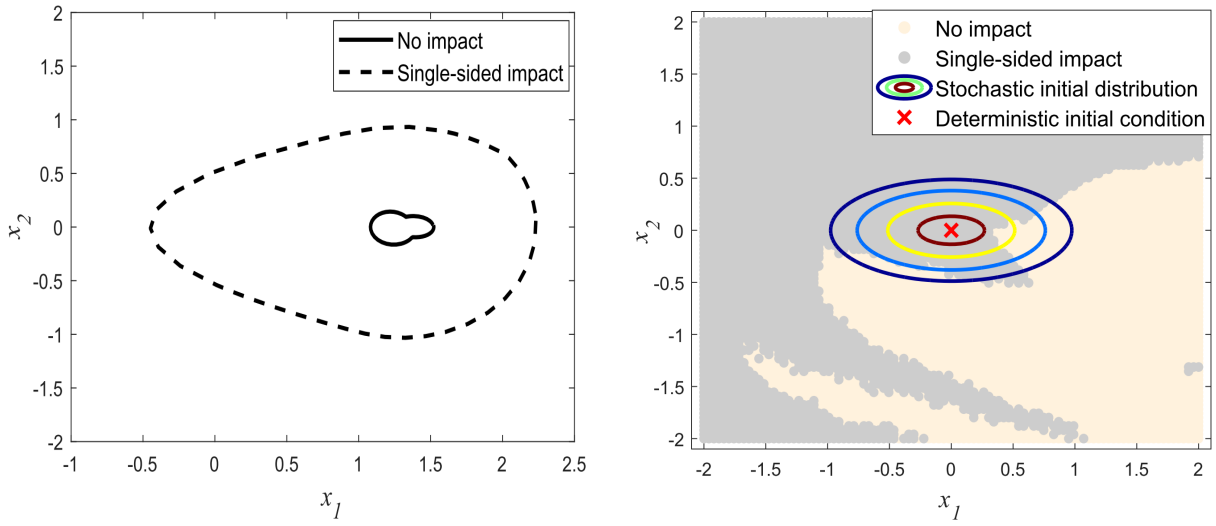

(a) (b)

Fig. 2. a) Multi-solution system with limit cycles in phase plane
b) Stochastic initial distribution versus deterministic initial condition in the domain of attraction of the system

5.2. Stochastic dynamics of 3D Problems

In order to investigate the effect of introducing noise spectrum on the probabilistic response of the gear model, three different stochastic excitations are considered here. The filter parameters for the three cases illustrated in Fig. 3 are specified in such a manner that the energy of the noise is kept constant. The intensity of noise for all cases of study is $\lambda = 0.05$.

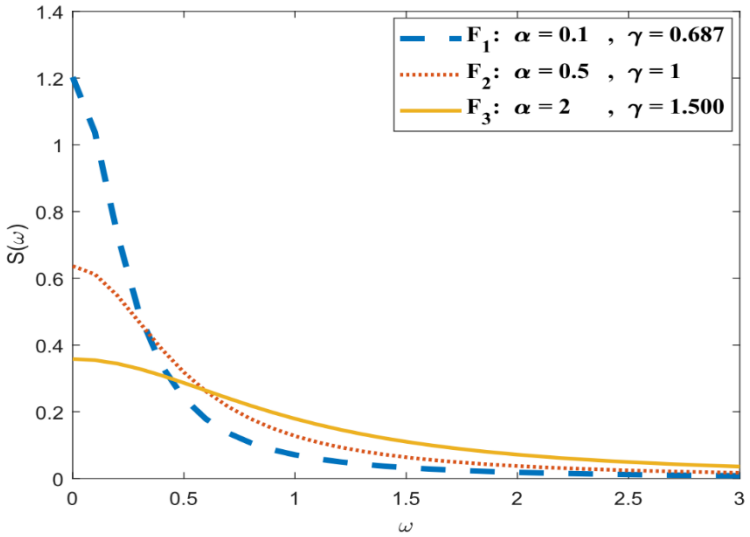

Fig. 3. Frequency spectrum for different noises

The first purpose of the current study is to show the capability of the adaptive path integration method to obtain accurate response PDF of a non-smooth random dynamical system under filtered noise. The evolution of the response PDF is captured via the PI technique with an adaptive time-stepping approach. Comparisons of the marginal PDFs for $t = 10t_p$ obtained by Monte Carlo simulations are shown in Figs 4-7 for cases A, B, C and D, respectively. The accuracy and precision of the method are confirmed qualitatively for all cases due to good agreement between the PI and MCS results. The difference between PI results and Monte Carlo simulations is more pronounced for cases C and D, since the variance of their PDF responses is smaller than cases A and B. Therefore, although our implementation of the path integration method in general seems to work very well, it may not be optimal for capturing with high accuracy the response of systems with very low variance.

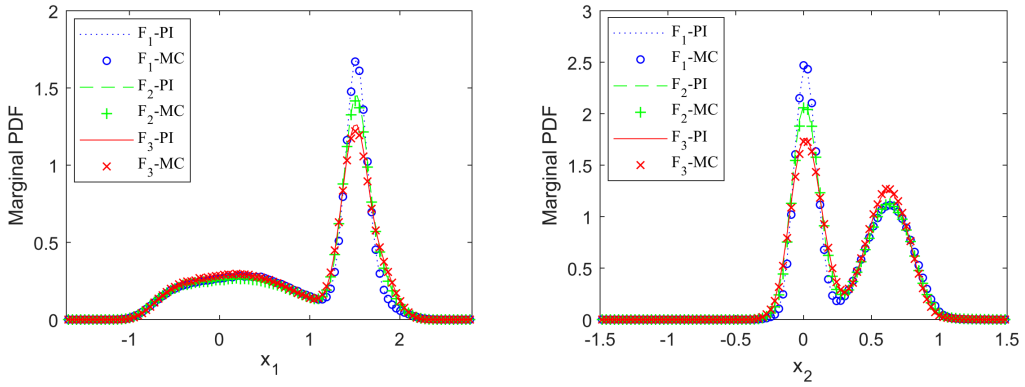

Fig. 4. Marginal PDFs of the response for case A after $10t_p$ obtained by the PI method and MC simulation

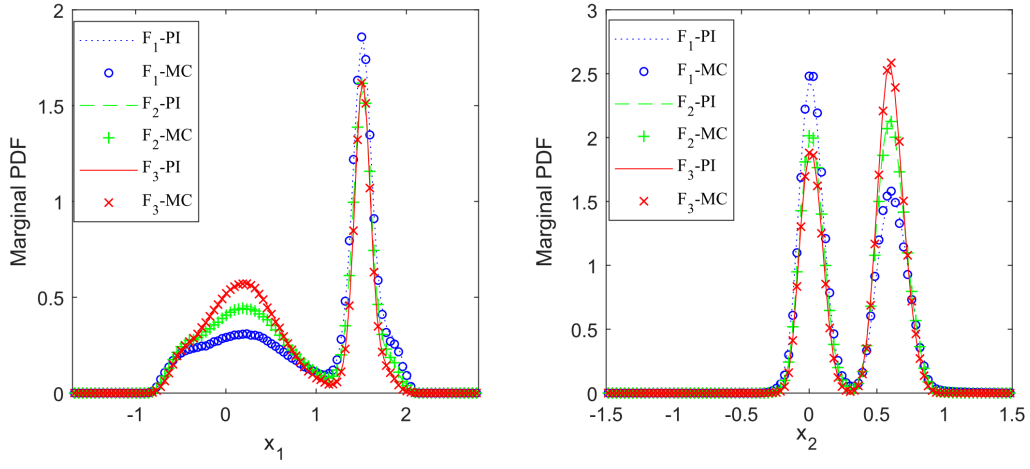

Fig. 5. Marginal PDFs of the response for case B after $10t_p$ obtained by the PI method and MC simulation

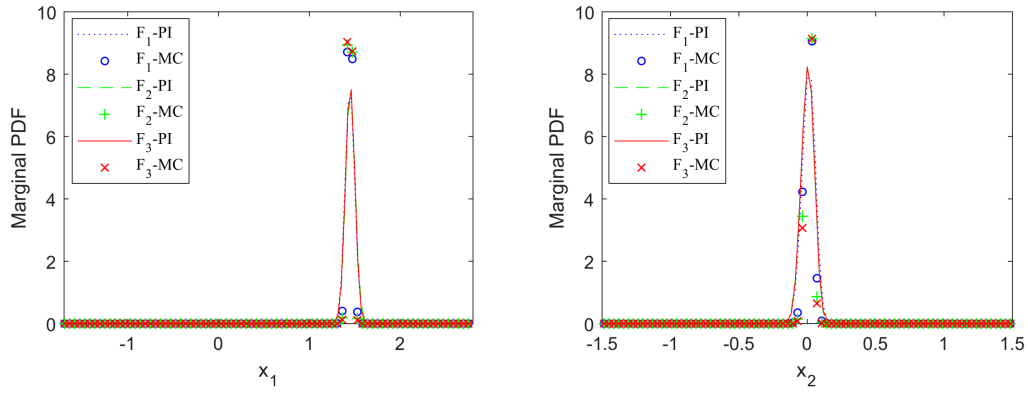

Fig. 6. Marginal PDFs of the response for case C after $10t_p$ obtained by the PI method and MC simulation

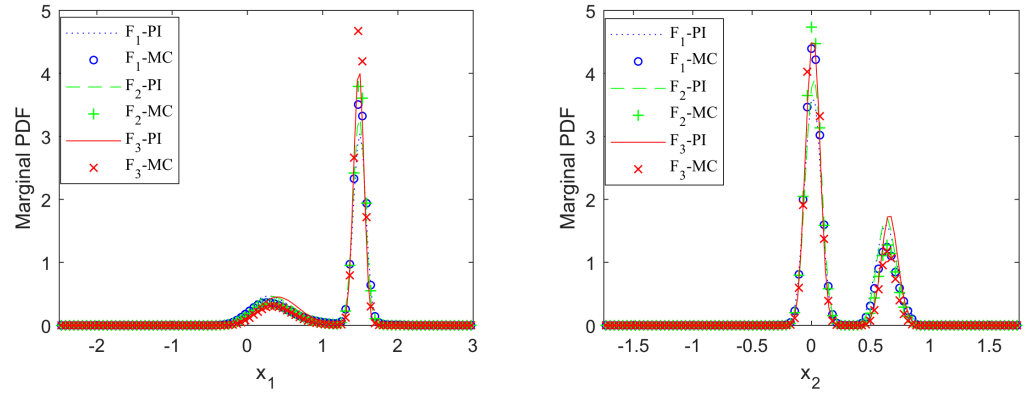

Fig. 7. Marginal PDFs of the response for case D after $10t_p$ obtained by the PI method and MC simulation

In order to better evaluate both the effects of noise spectrum and loading uncertainty, the joint PDFs are also plotted in Figs 8-11. In contrast to deterministic dynamic systems which assume a unique solution, the stochastic system response will be characterized by a probability distribution influenced by a nondeterministic distribution of initial conditions as well as an additive stochastic excitation In this study, the initial distribution covers both basins of attraction of each solution. According to similar studies [18,23], it is expected that both no-impact solutions and single-sided impact solutions coexist. However, in case C, it is seen that the stationary solution contains only the no-impact solution. It can be concluded that the uncertainty in frequency of an alternating load can unilaterally affect the domain of attraction. As the effect of uncertainty in these four categories reveals quite different results, the necessity of investigating the source of stochastic excitation in such nonlinear dynamical systems becomes obvious. It is also seen that the spectrum shape of the

additive noise partly affects the probabilistic response in cases A and B, while no significant effect is seen in cases C and D. Fig. 10 shows that the uncertainty in the rotational speed of the gear pair may significantly affect the inherent multi-solution behavior of the system.

The uncertainty in each component of the loading is basically due to external torque perturbations or manufacturing errors in the real system [28–30], but this matter is not pursued in the context of the current paper. The methodology and results that are presented in this study can have important implications in engineering applications of gear systems under uncertain excitation. The probability distribution function of the gear system response contains subtle information about the system, which is essential for the purpose of reliability-based design of such systems.

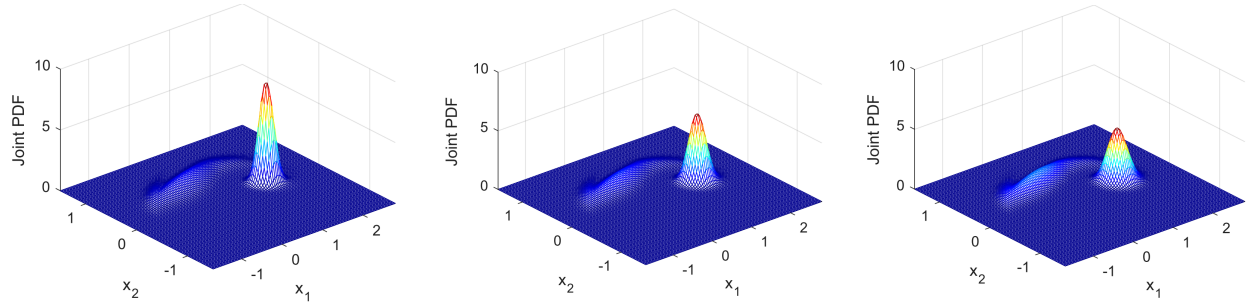

(a) (b) (c)

Fig. 8. Stationary response Joint PDF of the problem case A under filtered noise excitation of a) F_1, a) F_2 and c) F_3

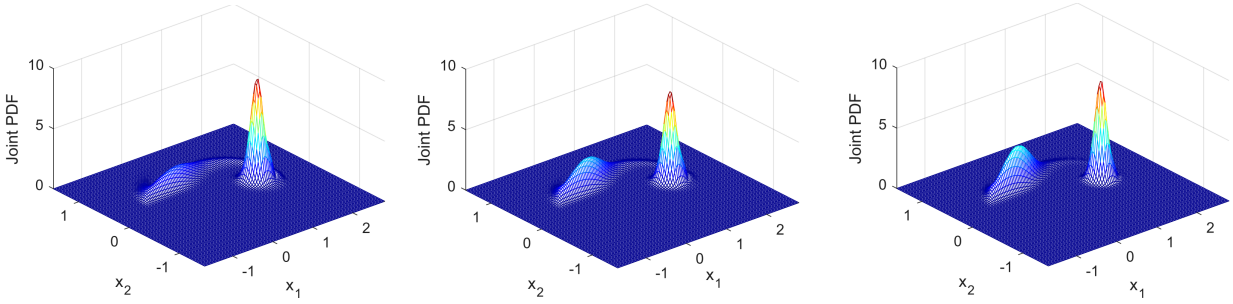

(a) (b) (c)

Fig. 9. Stationary response Joint PDF of the problem case B under filtered noise excitation of a) F_1, a) F_2 and c) F_3

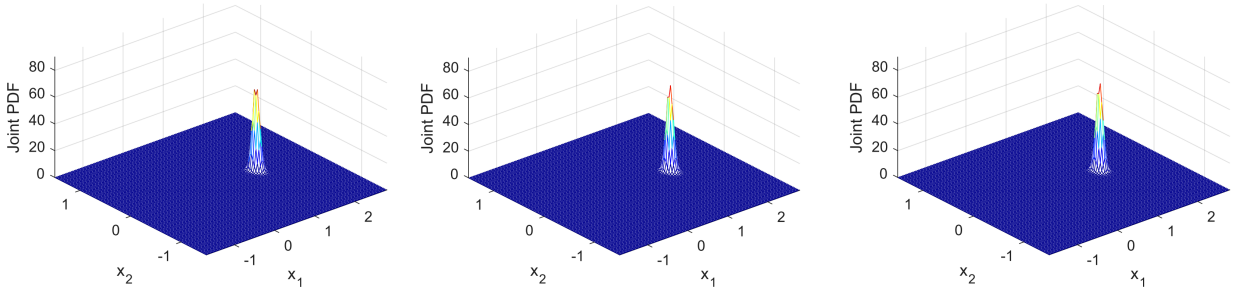

(a) (b) (c)

Fig. 10. Stationary response Joint PDF of the problem case C under filtered noise excitation of a) F_1, a) F_2 and c) F_3

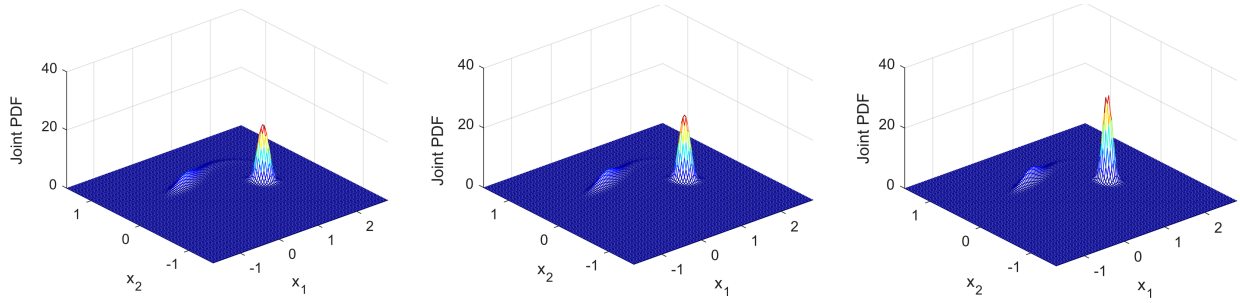

(a) (b) (c)

Fig. 11. Stationary response Joint PDF of the problem case D under filtered noise excitation of a) F_1, a) F_2 and c) F_3

5.3. Stochastic dynamics of the 4D Problem

Considering $\beta = 0.5$ and different parameter values for α and γ, the frequency spectrum of the equal-energy filtered noise is illustrated in Fig 12. These spectra can be considered as approximations of narrow-band noises with similar width but different peak. The intensity of the noise for all cases of this study is set to λ=0.05.

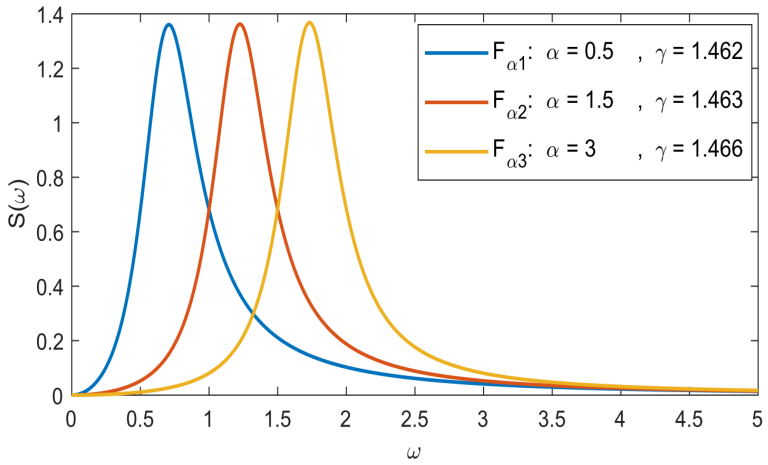

Fig. 12. Frequency spectrum of filtered noise with $\beta = 0.5$

The response PDF is calculated by the path integration method and compared with Monte Carlo simulations. Fig. 13-15 indicates marginal and joint PDFs of the response for $F_{\alpha 1}$, $F_{\alpha 2}$ and $F_{\alpha 3}$ at $t = 10t_p$.

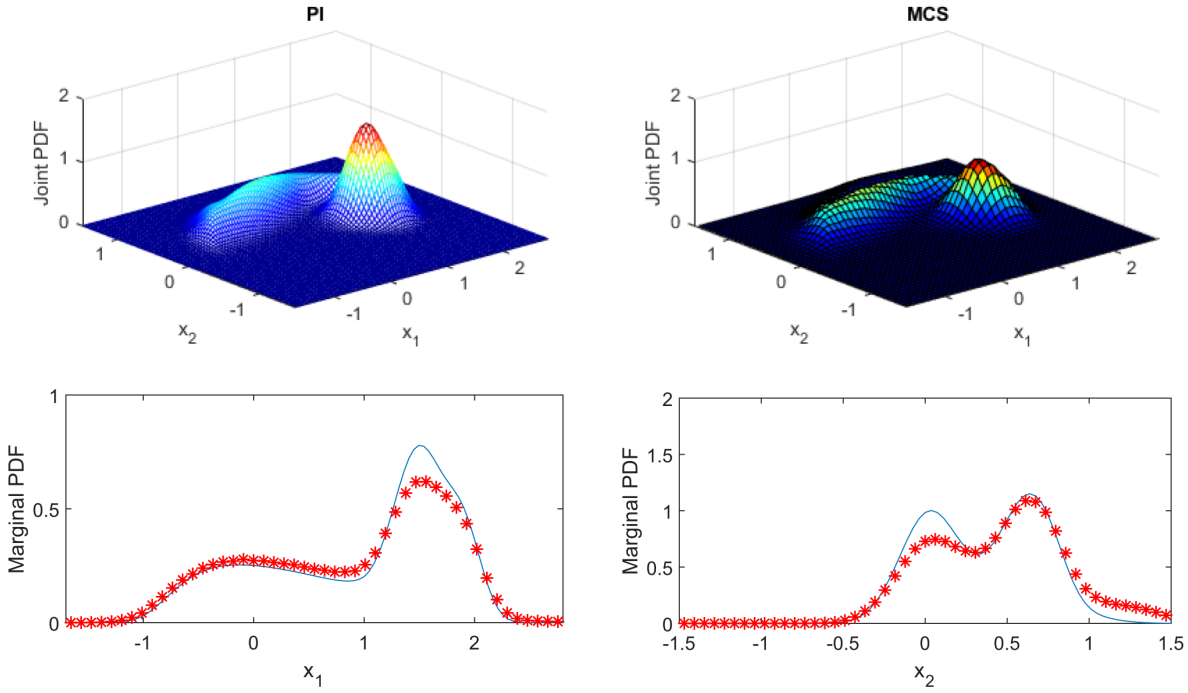

Fig. 13. Marginal and joint PDFs of the response for the 4D problem by the PI method and MCS for $F_{\alpha 1}$

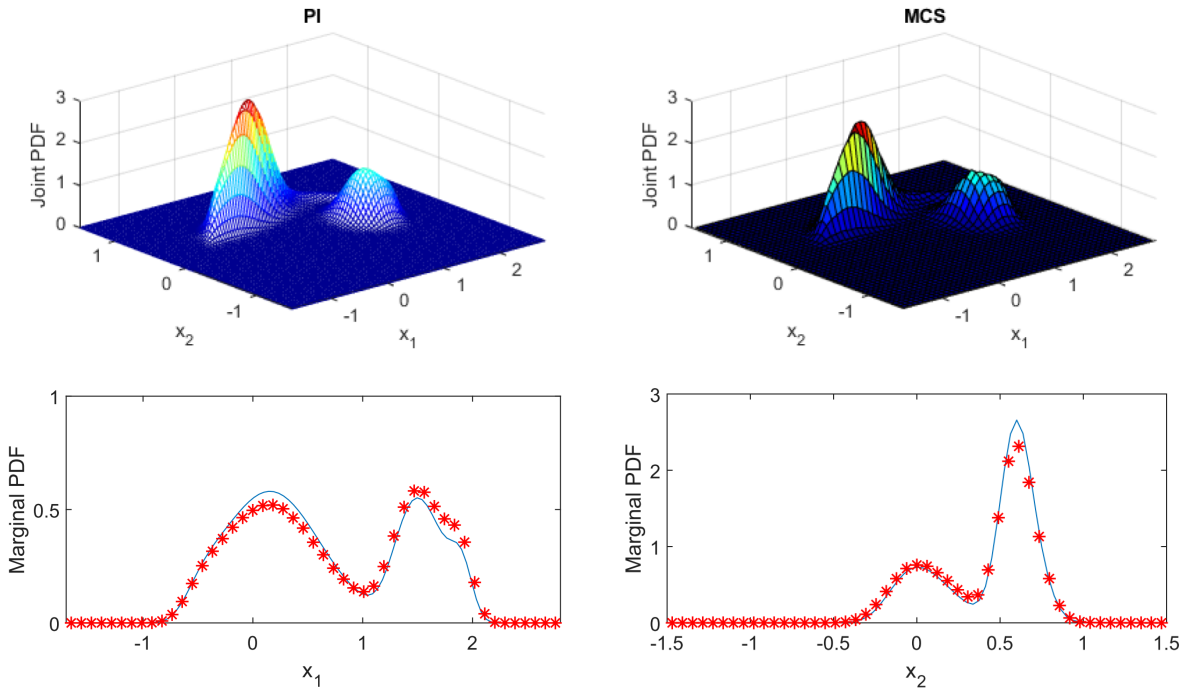

Fig. 14. Marginal and joint PDFs of the response for the 4D problem by the PI method and MCS for $F_{\alpha 2}$

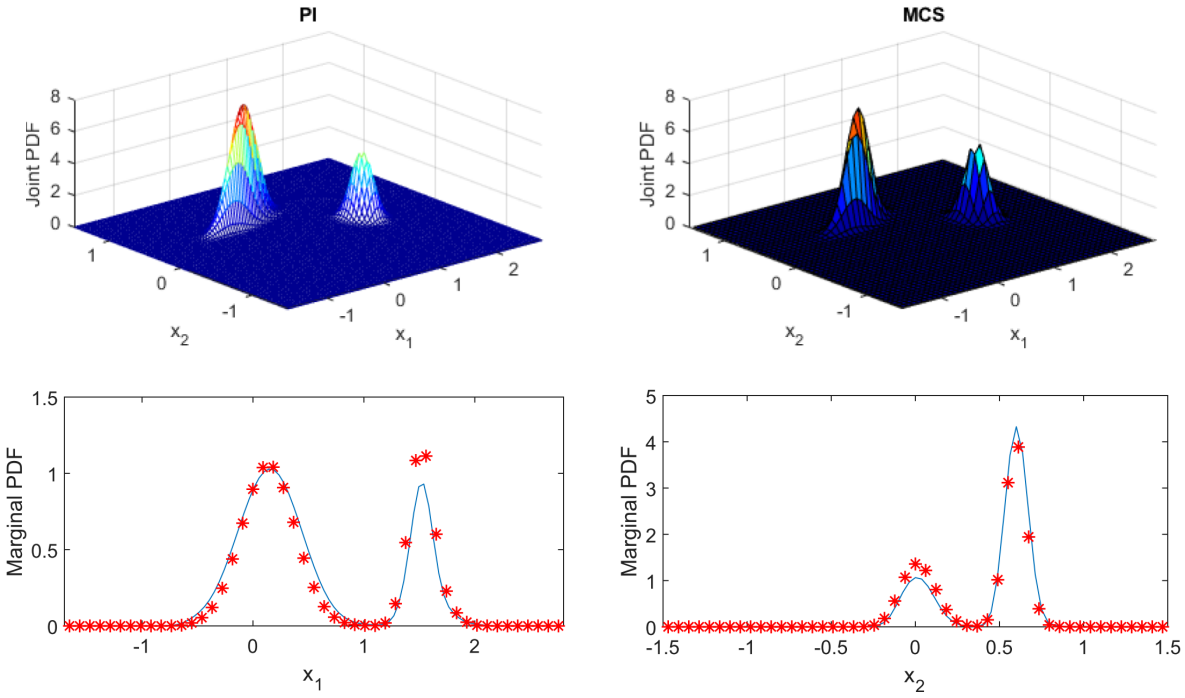

Fig. 15. Marginal and joint PDFs of the response for the 4D problem by the PI method and MCS for $F_{\alpha 3}$

Considering $\alpha = 1.5$ and different parameter values for α and γ, the frequency spectrum of the equal-energy filtered noise is illustrated in Fig 16. These spectra can be considered as approximations of narrow-band noises with similar peaks but different width.

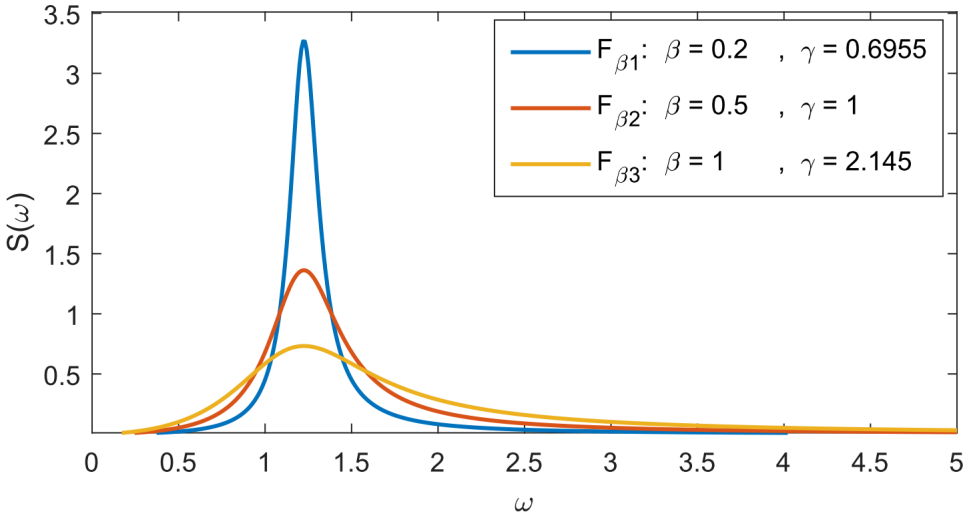

Fig. 16. Frequency spectrum of filtered noise with $\beta = 0.5$

The response PDF is calculated by the path integration method and compared with Monte Carlo simulations. Fig. 17-19 indicates marginal and joint PDFs of the response for $F_{\beta 1}$, $F_{\beta 2}$ and $F_{\beta 3}$ at $t = 10t_p$.

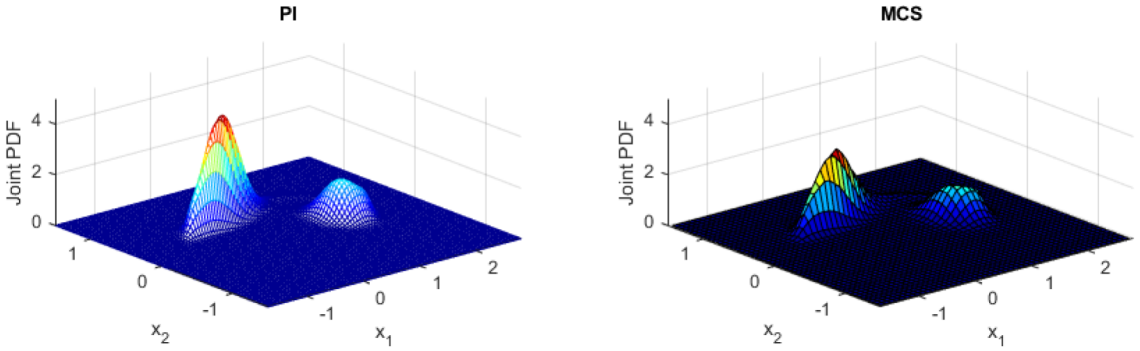

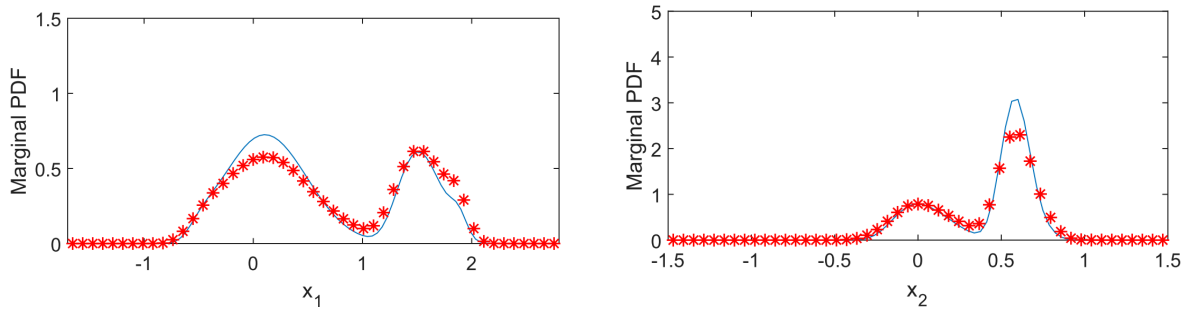

Fig. 17. Marginal and joint PDFs of the response for the 4D problem by the PI method and MCS for $F_{\beta 1}$

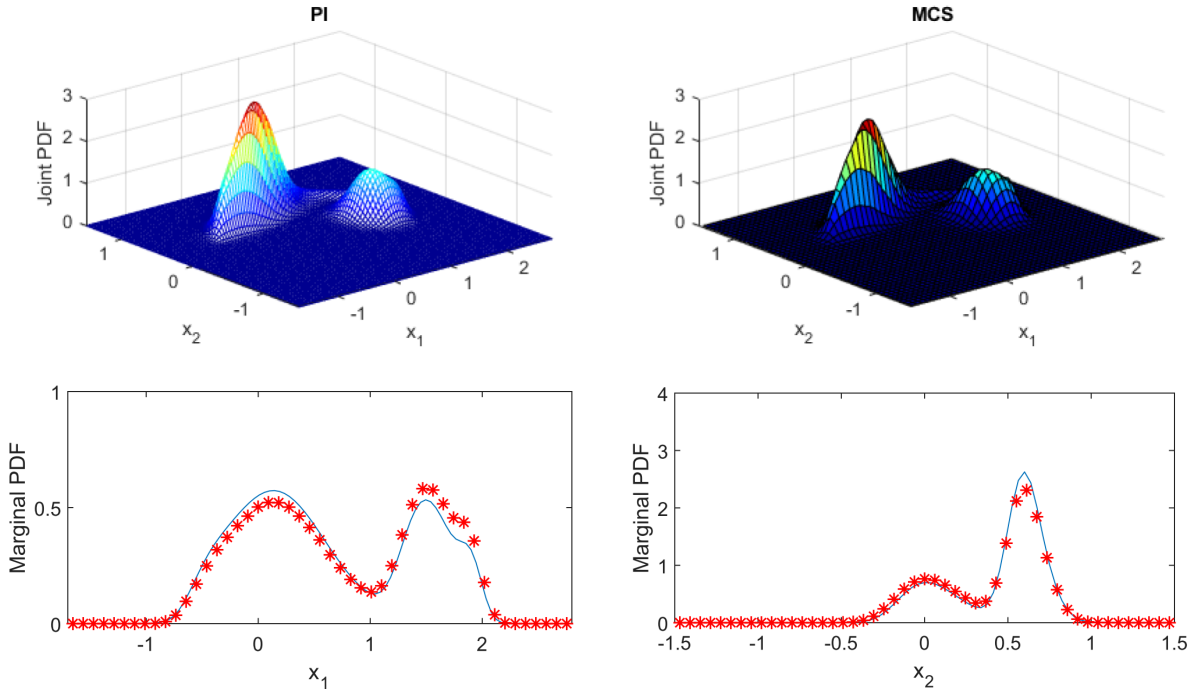

Fig. 18. Marginal and joint PDFs of the response for the 4D problem by the PI method and MCS for $F_{\beta 2}$

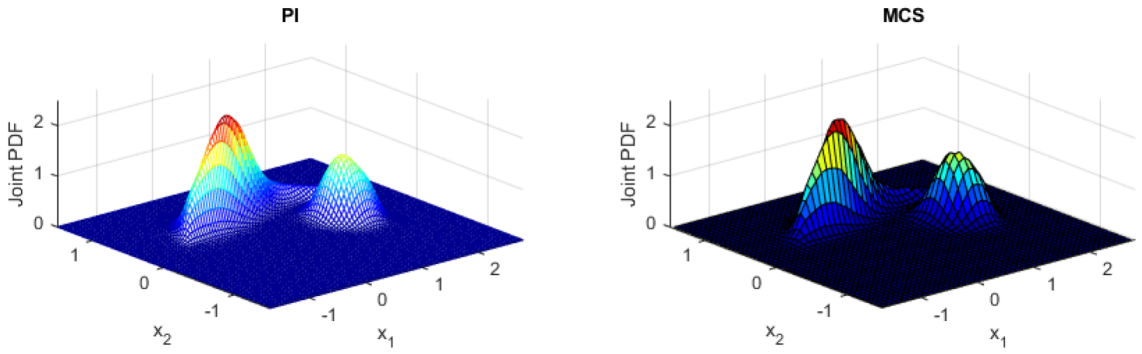

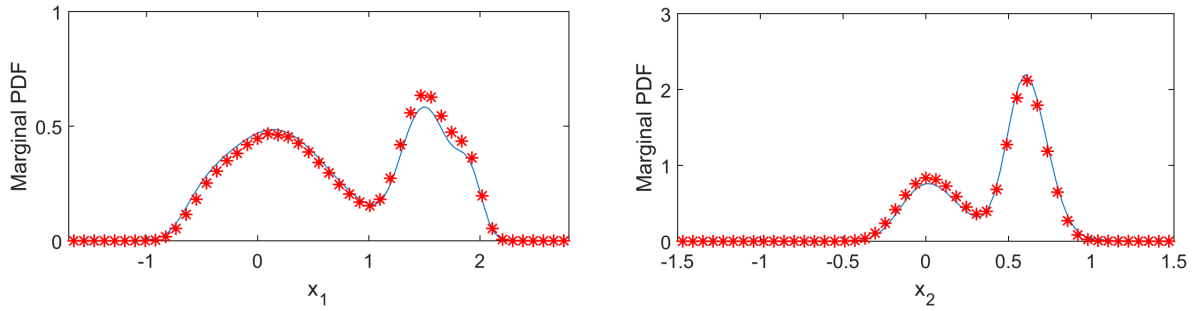

Fig. 19. Marginal and joint PDFs of the response for the 4D problem by the PI method and MCS for $F_{\beta 3}$

Although increasing the dimensions of the problem raised the computational cost, the accuracy and precision of the results are satisfactory for the solution of this non-smooth 4D problem. This shows the capability of the path integration method in dealing with higher dimensional problems of this type.

6. Conclusions

In the current study, the probabilistic response of a spur gear pair under uncertain loading is investigated. The single degree of freedom gear model contains both backlash nonlinearity and time-varying mesh stiffness. Based on which component of the loading contains uncertainty, four different sub-problems are defined. The uncertainty is assumed to be represented by a first order filtered white noise, resulting in a 3D state space problem. An efficient numerical path integration technique in combination with a novel adaptive time-stepping scheme is applied in order to capture accurately the evolution of the response PDF. Marginal PDFs calculated via the PI method are compared with those obtained by Monte Carlo simulations for each of the cases that are studied. The comparisons confirm the accuracy and precision of the methodology. The effect of uncertain loading on the stationary response is quite different depending on its origin. This demonstrates the importance of identifying the stochastic source in investigating the dynamics of gear systems. The effect of spectra on the dynamic behavior is also studied by considering three noise representations with equal energies but different frequency spectrum in each case. In addition, an extension of the problem to 4D, combining the gear model with a second order filter is investigated to show the capability of path integration method in dealing with higher dimensional problems. Parametric studies are carried out for the 4D problem. The response PDF contains raw but qualitatively important information that needs further interpretations according to the application.

Acknowledgments

We would like to express our gratitude to the Ministry of Science, Research and Technology of Iran and to the Norwegian University of Science and Technology (NTNU) for kindly providing an opportunity for S. Gheisari Hasnijeh to continue his research at NTNU as a visiting Ph.D. candidate. The contributions offered in discussions with Professor B. J. Leira and Dr. Wei Chai of NTNU are also highly appreciated.

Appendix – Derivation of the equation of motion

A semi-definite gear pair model with two degrees of freedom, as indicated in Fig. 1, is considered. The gears have rotary inertias and base circle diameters I_{gi} and d_{gi} respectively, and operate under input and output torques $\bar{T}_{gi}(\bar{t})$, $i = 1,2$. The equations of motion for this model are:

$$I_{g1}\frac{\mathrm{d}^2\theta_{g1}}{\mathrm{d}\bar{t}^2} + \frac{d_{g1}c_h}{2}\left(\frac{d_{g1}}{2}\frac{\mathrm{d}\theta_{g1}}{\mathrm{d}\bar{t}} - \frac{d_{g2}}{2}\frac{\mathrm{d}\theta_{g2}}{\mathrm{d}\bar{t}} - \frac{\mathrm{d}\bar{e}}{\mathrm{d}\bar{t}}\right) + \frac{d_{g1}}{2}\bar{f}\left(\frac{d_{g1}}{2}\theta_{g1} - \frac{d_{g2}}{2}\theta_{g2} - \bar{e}(\bar{t})\right) = \bar{T}_{g1}(\bar{t}) \qquad \text{(A1)}$$

$$I_{g2}\frac{\mathrm{d}^2\theta_{g2}}{\mathrm{d}\bar{t}^2} - \frac{d_{g2}c_h}{2}\left(\frac{d_{g1}}{2}\frac{\mathrm{d}\theta_{g1}}{\mathrm{d}\bar{t}} - \frac{d_{g2}}{2}\frac{\mathrm{d}\theta_{g2}}{\mathrm{d}\bar{t}} - \frac{\mathrm{d}\bar{e}}{\mathrm{d}\bar{t}}\right) - \frac{d_{g2}}{2}\bar{f}\left(\frac{d_{g1}}{2}\theta_{g1} - \frac{d_{g2}}{2}\theta_{g2} - \bar{e}(\bar{t})\right) = -\bar{T}_{g2}(\bar{t}) \qquad \text{(A2)}$$

where torques applied on the pinion and gear each includes three terms, namely, mean torque, fluctuating torque and additive noise: i.e., $\bar{T}_{g1}(\bar{t}) = \bar{T}_{g1m} + \bar{T}_{g1a}(\bar{t}) + \bar{T}_{g1w}(\bar{t})$ and $\bar{T}_{g2}(\bar{t}) = \bar{T}_{g2m} + \bar{T}_{g2a}(\bar{t}) + \bar{T}_{g2w}(\bar{t})$. The mesh elastic force $\bar{f}$ which is conceptually illustrated in Fig. 1, contains both time-varying mesh stiffness $k_h(\bar{t})$ and a nonlinear backlash function $f\big(\bar{q}(\bar{t})\big)$. The damping coefficient c_h is assumed to be constant which is accurate enough [3]. Equations (A1) and (A2) can be reduced to a single degree of freedom equation in terms of $\bar{q}(\bar{t})$ which is defined as the difference between the dynamic transmission error $\bar{x}(\bar{t})$ and the static transmission error $\bar{e}(\bar{t})$:

$$\bar{q}(\bar{t}) = \bar{x}(\bar{t}) - \bar{e}(\bar{t}) = \frac{d_{g1}}{2}\theta_{g1}(\bar{t}) - \frac{d_{g2}}{2}\theta_{g2}(\bar{t}) - \bar{e}(\bar{t}) \qquad \text{(A3)}$$

$$m_{c1}\frac{\mathrm{d}^2\bar{q}}{\mathrm{d}\bar{t}^2} + c_h\frac{\mathrm{d}\bar{q}}{\mathrm{d}\bar{t}} + k_h(\bar{t})f\big(\bar{q}(\bar{t})\big) = \bar{F}_m + \bar{F}_{aT}(\bar{t}) + \bar{F}_{ah}(\bar{t}) + \bar{F}_W(\bar{t}) \qquad \text{(A4)}$$

$$m_{c1} = \frac{4\, I_{g1} I_{g2}}{{d_{g2}}^2 I_{g1} + {d_{g1}}^2 I_{g2}} \quad , \quad m_{c2} = \frac{4 I_{g1}}{d_{g1}} \quad , \quad m_{c3} = \frac{4 I_{g2}}{d_{g2}} \tag{A5a-c}$$

$$\bar{F}_m = \frac{2\bar{T}_{g1m}}{d_{g1}} = \frac{2\bar{T}_{g2m}}{d_{g2}} \quad , \quad \bar{F}_{aT}(\bar{t}) = \frac{2m_{c1}\bar{T}_{g1a}(\bar{t})}{m_{c2}} + \frac{2m_{c1}\bar{T}_{g2a}(\bar{t})}{m_{c3}} \tag{A6, A7}$$

$$\bar{F}_{ah}(\bar{t}) = -m_{c1}\frac{\mathrm{d}^2\bar{e}}{\mathrm{d}\bar{t}^2} \quad , \quad \bar{F}_W(\bar{t}) = \frac{2m_{c1}\bar{T}_{g1w}(\bar{t})}{m_{c2}} + \frac{2m_{c1}\bar{T}_{g2w}(\bar{t})}{m_{c3}} \tag{A8, A9}$$

$$f\big(\bar{q}(\bar{t})\big) = \frac{\bar{f}\big(\bar{q}(\bar{t})\big)}{k_h(\bar{t})} = \begin{cases} \bar{q}(\bar{t}) - b & \bar{q}(\bar{t}) > b \\ 0 & -b < \bar{q}(\bar{t}) < b \\ \bar{q}(\bar{t}) + b & \bar{q}(\bar{t}) < -b \end{cases} \tag{A10}$$

where $2b$ is the backlash for the gears in the mesh. The dimensionless form of (A3) can be obtained by defining $\omega_n = \sqrt{k_{hm}/m_{c1}}$, $t_p = 1/\omega_n$, $q(\bar{t}) = \bar{q}(\bar{t})/b$, $t = \omega_n \bar{t}$ and $\zeta = c_h/(2m_{c1}\omega_n)$, where k_{hm} is the average mesh stiffness and is only used to non-dimensionalize the equation of motion. For the sake of simplicity, the external excitation $\bar{F}_{aT}(\bar{t})$ is neglected. Considering dimensionless quantities for the mesh frequency $\Omega_h = \bar{\Omega}_h/\omega_n$, the mean loading becomes $F_m = \bar{F}_m/(bk_{hm})$, the fluctuating loading $F_{ah} = \bar{F}_{ah}/(bk_{hm})$, the stochastic loading $F_W(\bar{t}) = \bar{F}_W/(bk_{hm})$, the time-varying mesh stiffness $k(t) = k_h(\bar{t})/k_{hm}$ and the static transmission error $e = \bar{e}/b$. The following equation of motion is then obtained [2]:

$$\ddot{q}(t) + 2\zeta\dot{q}(t) + k_h(t) f\big(q(t)\big) = F_m + F_{ah}{\Omega_h}^2 \cos(\Omega_h t) + F_W(t) \tag{A11}$$

$$f\big(q(t)\big) = \begin{cases} q(t) - 1 & q(t) > 1 \\ 0 & -1 < q(t) < 1 \\ q(t) + 1 & q(t) < -1 \end{cases} \tag{A12}$$

References

[1] H.N. Ozguven, D.R. Houser, Mathematical models used in gear dynamics—A review, J. Sound Vib. 121 (1988) 383–411.

[2] A. Kahraman, R. Singh, Non-linear dynamics of a spur gear Pair, J. Sound Vib. 142 (1990) 49–75.

[3] A. Kahraman, R. Singh, Interactions between time-varying mesh stiffness and clearance non-linearities in a geared system, J. Sound Vib. 146 (1991) 135–156.

[4] G.W. Blankenship, A. Kahraman, Steady state forced response of a mechanical oscillator with combined parametric excitation and clearance type non-linearity, J. Sound Vib. 185 (1995) 743–765. doi:10.1006/jsvi.1995.0416.

[5] R.G. Parker, S.M. Vijayakar, T. Imajo, Non-Linear Dynamic Response of a Spur Gear Pair: Modelling and Experimental Comparisons, J. Sound Vib. 237 (2000) 435–455.

[6] C.G. Cooley, R.G. Parker, A Review of Planetary and Epicyclic Gear Dynamics and Vibrations Research, Appl. Mech. Rev. 66 (2014) 1–15. doi:10.1115/1.4027812.

[7] H. Ma, J. Zeng, R. Feng, X. Pang, Q. Wang, B. Wen, Review on dynamics of cracked gear systems, Eng. Fail. Anal. 55 (2015) 224–245. doi:10.1016/j.engfailanal.2015.06.004.

[8] E. Goβmann, H. Waller., Analysis of multi-correlated wind , excited vibrations of structures using the covariance method, Eng. Struct. 5 (1983) 264–272.

[9] T.K. Caughey, Nonlinear Theory of Random Vibrations, Adv. Appl. Mech. 11 (1971) 209–253.

[10] T. Tobe, K. Sato, N. Takatsu, Statistical analysis of dynamic loads on spur gear teeth: effect of shaft stiffness, Bull. JSME. 19 (1976) 808–813.

[11] T. Tobe, K. Sato, N. Takatsu, Statistical analysis of dynamic loads on spur gear teeth (Experimental Study), Bull. JSME. 20 (1977) 1315–1320.

[12] A.S. Kumar, M.O.M. Osman, T.S. Sankar, On Statistical Analysis of Gear Dynamic Loads, J. Vib. Acoust. Stress. Reliab. Des. 108 (1986) 362–368.

[13] S. V. Neriya, R.B. Bhat, T.S. Sankar, On the Dynamic Response of a Helical Geared System Subjected to a Static Transmission Error in the Form of Deterministic and Filtered White Noise Inputs, J. Vib. Acoust. Stress. Reliab. Des. 110 (1988) 501–506.

[14] F. Pfeiffer, A. Kunert, Rattling models from deterministic to stochastic processes, Nonlinear Dyn. 1 (1990) 63–74.

[15] Y. Wang, W.J. Zhang, Stochastic vibration model of gear transmission systems considering speed-dependent random errors, Nonlinear Dyn. 17 (1998) 187–203.

[16] M.F. Wehner, W.G. Wolfer, Numerical evaluation of path-integral solutions to Fokker-Planck equations, Phys. Rev. A. 27 (1983) 2663–2670.

[17] A. Naess, V. Moe, Efficient path integration methods for nonlinear dynamic systems, Probabilistic Eng. Mech. 15 (2000) 221–231.

[18] J.S. Yu, Y.-K.K. Lin, Numerical path integration of a non-homogeneous Markov process, Int. J. Non. Linear. Mech. 39 (2004) 1493–1500.

[19] H.T. Zhu, Non-stationary response of a van der Pol-Duffing oscillator under Gaussian white noise, Meccanica. 52 (2016) 833–847.

[20] A. Naess, F.E. Kolnes, E. Mo, Stochastic spur gear dynamics by numerical path integration, J. Sound Vib. 302 (2007) 936–950.

[21] J.Q. Sun, C.S. Hsu, The Generalized Cell Mapping Method in Nonlinear Random Vibration Based Upon Short-Time Gaussian Approximation, J. Appl. Mech. 57 (1990) 1018–1025.

[22] E. Mo, A. Naess, Nonsmooth Dynamics by Path Integration: An Example of Stochastic and Chaotic Response of a Meshing Gear Pair, J. Comput. Nonlinear Dyn. 4 (2009) 34501.

[23] Y. Wen, J. Yang, S. Wang, Random dynamics of a nonlinear spur gear pair in probabilistic domain, J. Sound Vib. 333 (2014) 5030–5041.

[24] S.G. Hasnijeh, M. Poursina, B.J. Leira, H. Karimpour, W. Chai, Stochastic dynamics of a nonlinear time-varying spur gear model using an adaptive time-stepping path integration method, J. Sound Vib. 447 (2019).

[25] A.F. Psaros, O. Brudastova, G. Malara, I.A. Kougioumtzoglou, Wiener Path Integral based response determination of nonlinear systems subject to non-white, non-Gaussian, and non-stationary stochastic excitation, J. Sound Vib. 433 (2018) 314–333. doi:10.1016/j.jsv.2018.07.013.

[26] I.A. Kougioumtzoglou, P.D. Spanos, An analytical Wiener path integral technique for non-stationary response determination of nonlinear oscillators, Probabilistic Eng. Mech. 28 (2012) 125–131. doi:10.1016/j.probengmech.2011.08.022.

[27] Y. Fang, X. Liang, M.J. Zuo, Effects of friction and stochastic load on transient characteristics of a spur gear pair, Nonlinear Dyn. 93 (2018) 1–11.

[28] J.H. Kuang, A.D. Lin, Theoretical aspects of torque responses in spur gearing due to mesh stiffness variation, Mech. Syst. Signal Process. 17 (2003) 255–271.

[29] M. Inalpolat, A Computational Model to Investigate the Influence of Spacing Errors on Spur Gear Pair Dynamics, in: Exp. Tech. Rotating Mach. Acoust., Springer, Cham, 2015: pp. 1–10.

[30] E.P. Remmers, Gear mesh excitation spectra for arbitrary tooth spacing errors, load and design contact ratio, J. Mech. Des. 100 (1978) 715–722.

[31] W. Chai, A. Naess, B.J. Leira, Filter models for prediction of stochastic ship roll response, Probabilistic Eng. Mech. 41 (2015) 104–114.

[32] E. Mo, Nonlinear stochastic dynamics and chaos by numerical path integration, PhD Thesis, Norwegian University of Science and Technology, 2008.

[33] P.E. Kloeden, E. Platen, Numerical solution of stochastic differential equations, Springer-Verlag, 1992.

[34] A. Naess, J.M. Johnsen, Response statistics of nonlinear, compliant offshore structures by the path integral solution method, Probabilistic Eng. Mech. 8 (1993) 91–106.